HOSTED BY
ELSEVIER
CrossMark
Available online at www.sciencedirect.com
ScienceDirect
Biosurface and Biotribology 3 (2017) 135–143
www.elsevier.com/locate/bsbt

Does silica concentration and phytolith ultrastructure relate to phytolith hardness?

Ellen Schulz-Kornas[a,b,*], Caroline Braune[b], Daniela E. Winkler[b,c], Thomas M. Kaiser[b]

[a]*Max Planck Weizmann Center for Integrative Archaeology and Anthropology, Max Planck Institute for Evolutionary Anthropology, Deutscher Platz 6, 04103 Leipzig, Germany*
[b]*Center of Natural History, University of Hamburg, Martin-Luther-King-Platz 3, 20146 Hamburg, Germany*
[c]*Institute of Geosciences, Johannes Gutenberg-University Mainz, J.-J.-Becher-Weg 21, 55128 Mainz, Germany*

Received 28 September 2017; received in revised form 5 December 2017; accepted 26 December 2017

Abstract

Grasses are an important part of the forage of many herbivorous mammals and their phytoliths have long been regarded as the most important agent of tooth wear. Recent work has challenged this "paradigm" in finding evidence 1. of native phytoliths to be much softer then tooth enamel and 2. indicating, that phytolith hardness is highly variable, 3. prone to methodology and 4. not easy to be related to habitat conditions. We conduct controlled silica-cultivations measuring SiO_2 content in the common forage grass *Themeda triandra*. Phytoliths are extracted natively, and nano-indentation values are measured. Phytolith hardness in *Themeda triandra* is found to be independent of silicate availability in the substrate. We further investigate the phytolith ultrastructure of *Hordeum vulgare* phytoliths. Phytoliths are shown to be an anisotropic composite of at least 3 components, silica bodies, inter-body matrix (both mineralised) and globular inclusions (likely non-mineralised). It can be argued, that indentation will be largely influenced by the heterogeneity of the structure and thus nano-indentation measurements will largely reflect the matrix and its mechanical properties but not necessarily the silicate bodies, which make up the vast majority of a phytolith.

Keywords: Phytolith; Indentation; Ultrastructure; Material property; Silicate availability; Tooth wear

1. Introduction

Tooth morphology and tooth wear of herbivorous mammals has long been used for the interpretation of dietary behaviour and habitat reconstruction [1–4]. As grasses (Poaceae) constitute a significant proportion of the ingesta of many herbivorous mammals, their mineral inclusions (especially phytoliths) have long been assumed to be the main cause of tooth-wear [e. g. 5] and could be a powerful plant defense mechanism induced by herbivory [6–10] and do wear enamel [11]. This topic is highly discussed [12–15] and some studies, however, question this hypothesis because various methods of hardness tests indicating that opal phytoliths are softer then tooth enamel [16–20]. Lucas et al. [21] found the indentation hardness of enamel to be about 5 GPa, but significantly lower values were given for phytolits (0.9 GPa squash, 2.5 GPa grass), higher values for quartz dust. It is often assumed that external abrasives are the more important tooth wear agents in grazing mammals compared to phytoliths, because external abrasives are ingested in large amounts. Highest values for external abrasives from soil consumption are found for mammals with a grazing feeding behavior like in the domestic sheep in New Zealand which are showing peak soil intakes of 33% of daily dry matter intake (DMI, [22–25]). However, annual average soil intake values for sheep tend to range of 5–9% [22–26] and are comparable with other grazing ungulates (like the bison 6.8% [27]), grazing perissodactyles (like the feral horse 5%; [28]), while primary large African browsing species

*Corresponding author at: Max Planck Weizmann Center for Integrative Archaeology and Anthropology, Max Planck Institute for Evolutionary Anthropology, Deutscher Platz 6, 04103 Leipzig, Germany.
E-mail addresses: ellen_schulz@eva.mpg.de (E. Schulz-Kornas), carolinebraune@gmx.de (C. Braune), dawinkle@uni-mainz.de (D.E. Winkler), thomas.kaiser@uni-hamburg.de (T.M. Kaiser).
Peer review under responsibility of Southwest Jiaotong University.

http://dx.doi.org/10.1016/j.bsbt.2017.12.004

have soil intake rates below 5% faecal DMI with grazers tending to have higher values of 5.2–16.3% faecal DMI than browsers [29]. For internal abrasives like phytoliths such values are unknown. A thorough understanding of phytolith ultrastructure as well as their mechanical properties can be seen as a first step towards better comprehending their role during the mechanical disintegration of food particles.

Determining the mechanical properties of biogenic materials, such as opal phytoliths, is a challenging task. It is of high relevance in biotribolgical research requiring material testing on morphologically dissimilar biological particles involved in the wear process at nano-meter scale and is therefore of interest for many research disciplines like engineering, life sciences, veterinary medicine as well as anthropology, archaeology and palaeontology.

In general the amorphous mineral silica (opal) is commonly present in many plants and animals [30,31]. However, opal phytolith formation itself is poorly understood. In this pilot study, we use the term phytolith exclusively for silicate-containing plant bodies called opal-phytoliths. Former phytolith studies [5,16,18] provide little information about the origin of the plant material used and details of indentation measurements, which makes their results hard to compare. The only studies describing silicate uptake and phytolith ultrastructure and inferring on the process of phytolith formation are Kaufman, et al. [32], Kaufman, et al. [33], who describe the polymerization of silicate as follows: silicic acid is irreversibly formed to amorphous silicate gel (SiO_2*nH_2O), a non-crystalline product that has a hydrophobic SiO_2-molecule with corresponding hydrophilic OH groups at the surface. They present four levels of the silification process of phytoliths in *Avena sativa* L. In the interphase of intercalary meristem cells of an internode a sequence of long and short cells arises. The short cells can develop into a pair of silica and cork cell, stomata cells or trichomes. In the first stage of silification a short cell splits into a pair of cells, the future silica cell and the cork cell that initially appear morphologically similar. In the second stage, the two cells differentiate in size and shape. In the third stage, the nucleus of the future silica cell perishes and silicate is entering the final stage.

At the degradation of the nucleus, fibrillar elements arise from this and other cytoplasmic elements that spread through the cell lumen. The only remaining organelles are dark osmiophilic droplets, which are potentially derived from lipid droplets. Further, Kaufman, et al. [32] describe thickened cell walls forming around the cork and silica cell. The silica bodies now growing into the cell lumen of the silica cell are non-crystalline (containing 13.5% bound water) and are interpreted as silica gel. They grow along the fibrillar elements in parallel prism-like bodies [32].

1.1. Phytolith hardness and silicate concentration

If phytolith hardness would be only determined by the limited availability of silica cells produced by the apical meristem, one should assume that the silicate concentration available to plants in the soil had no effect on the hardness of phytoliths. The latter would then be independent of growth site and soil composition. Later in the ontogeny of a silica cell [32], barriers in its cytoplasma membrane account for a stop of further silica deposition in the cell. There is, however, good evidence, that once the apical meristem is removed (e.g. by feeding herbivores), resting mersitems are activated, which subsequently cause lateral growth including further silica deposition [34]. This growth pattern may account for the observation that pastures under high feeding pressure tend to show increased silica contents, which widely has been interpreted as a possible effect of animal-plant interaction causing increases in tooth wear [35]. In detail it has been shown the number, shape and distribution of Si-rich phytoliths and spines differ within and between different grass species and demonstrate that species also differ in their ability to change the deposition and distribution of these defenses in response to damage or increases in Si supply [9,36,37]. This would lead to an increased over all abrasiveness would thus be related to the proportion of silica phytoliths in ingesta, but would be independent of phytolith hardness. In a global sense, the evolution of herbivory may not be considered independent of phytolith hardness, because tooth abrasion is crucial to any vertebrate and to mammals in particular. A yet unsolved question is if phytolith hardness is independent of biogeographic parameters (such as silicate availability). If not so, we suggest that herbivore biogeography may have to be reconsidered as a result of differential abrasive impacts of herbivorous diets.

To test for a possible relationship between silicate concentration in the soil and the material properties of phytoliths, we determine the hardness of native opal phytoliths of *Themeda triandra* FORSSK. grown on a silicate-controlled cultivation with 10 and 100 mg SiO_2/L. The specific material properties of phytoliths are widely enigmatic, we chose to apply a standardised nano-indentation measurement (DIN EN ISO 145677) using the CSM-technique. This approach allows extracting material properties of the tested particles in a specific indentation depth and can therefore also reliably describe inhomogenous ultrastructures. We use *Themeda triandra* as a focal phytolith species because it is a common forage plant by a wide range of herbivorous mammals such as wildebeest, zebra [38–40], Grant's gazelle, Thomson's gazelle [40], zebu [38,40] and hartebeest [38].

Aside from nano-indentation measurements, the interpretation of phytolith biomechanical properties requires knowledge of phytolith-formation in silicate-accumulating plants, as well as ultrastructural information on phytoliths. A further aim of this pilot study is therefore to investigate the internal structure of phytoliths and improve the understanding of phytolith formation. We thus perform transmission electron microscopy (TEM) analyses of phytoliths of *Hordeum vulgare* L., which originate from a silicate-controlled cultivation (100 mg SiO_2/L). We choose *Hordeum vulgare* because it produces long-epidermal cell phytoliths particularly suitable for ultra thin sectioning because of their elongated morphology.

2. Material and methods

2.1. Silicate controlled cultivation and phytolith extraction

Silicate-controlled cultivations of *Themeda triandra* [red grass] with 10 and 100 mg SiO_2/L and *Hordeum vulgare* [barley] with

100 mg SiO_2/L were carried out during the summer months of 2011 at the Biocenter Klein Flottbek and Botanical Garden of the University of Hamburg (Germany). Seeds for were provided from KPR Gardeners Club (Slovakia; red grass) and IPK (Leibnitz-Institut für Pflanzengenetik und Kulturpflanzenforschung, OT Gatersleben, Stadt Seeland, Germany; barley).

Perforated boxes (50 × 32 × 6 cm) were placed on irrigation mats and filled with 5 cm coconut fibre substrate (Baldur, Bensheim, Germany). A second irrigation mat was placed on top of the coconut fibre, on which then the seeds were spread. The irrigation mats were saturated with desalinated water. The seeds were also carefully sprinkled with desalinated water using a plant sprayer. The seeds were covered with evaporation protection boxes until the seedlings had reached a size of 5 cm.

After 7 days, the cultivation was manually irrigated with 1–2 l twice per week. Excess water could escape through a drain; hence the root system was protected from oxygen deficiency due to standing water. The nutrient composition from Braune, et al. [41] was slightly modified: Cobalt(II)nitrate hexahydrate ($Co(NO_3)_2$*$6H_2O$) was replaced by Cobalt(II)chloride hexahydrate ($CoCl_2$*$6H_2O$). 1 L stock solution was prepared according to Braune et al. [41]. Iron, as EDTA-iron(III)sodium salt hydrate (36.7 mg/L), and silicate, as sodium silicate SiO_2:Na_2O_3 (3.7 g for 10 mg SiO_2, 37 g for 100 mg SiO_2), were added to the working solution (1/10 of the stock solution). A *Bacillus thuringiensis israelensis* solution (1 mL/L, Neudomück, W. Neudorff GmbH KG, Emmerthal, Germany) was added to the working solution to protect against mosquito larvae infestation. The pH was adjusted with hydrochloric acid and sodium hydroxide solution to 5.8–6.0. The plants were harvested after 83 days and subsequently packed and stored at −20 °C.

Phytolith extraction from the biomass (leaves and steams) was performed using the the water-boiling method at 100 °C as described in Braune et al. [41]. Therefore our approach is less prone to changes of material properties of phytoliths thru high temperature during the extraction process using dry ashing with temperatures used above 400 °C [42–44]. The extracted samples of *T. triandra* were embedded in epoxy resin and polished following Kaiser, et al. [17].

2.2. Measuring nano-indentation

Nano-indentation was performed on 9 phytoliths of *Themeda triandra* (Fig. 1a) from the 10 mg SiO_2/L population and 12 phytoliths from the 100 mg SiO_2/L population (Fig. 1e). A microscopic slide (c) used to support phytoliths for indentation measuring (Fig. 1c).). Phytoliths are glued to the slide via a thin layer of epoxy resin. Nano-indentation measurements were carried out with a nanoindenter XP (Agilent Technologies, Santa Clara, USA) with a Berkovich-diamond-indenter according to DIN EN ISO 14577 using the continuous stiffness measurement (CSM) option. With this option, a small additional oscillating force is superimposed to the main load ramp. Due to the separation of in-phase and out-of-phase components of the load-displacement hysteresis, the initial contact between tip and surface can be determined accurately. Furthermore, since the contact stiffness is determined continuously during the main loading ramp, any change of stiffness during the complete test can be detected. Thus, the force range for stiffness evaluation of an indented particle below the force where sink-in occurs can be determined for each indent individually.The indentation-curves were checked visually over a range of 600 nm indentation depth and showed plateaus in different areas. These plateaus in the indentation depth were individual determined for the 2–4 indents for each phytolith (Table 1). Indentation depths of these ranges were averaged and included in the statistical analysis.

2.3. Statistical analysis

All statistics were conducted in R (version 2.13.2, R Team [45]). The following R packages were used: 'R Core Team' and 'doBy' (version 4.2.3, Højsgaard, et al. [46]), R.utils (version 1.6.2, Bengtsson [47]), RSvgDevice (version 0.6.4.1, Luciani [48]), and xlsReadWrite (Version 1.5.4, Suter [49]). We further employ the software package WRS (Wilcox and Schönbrodt [50]) and use features of Wilcox [51]. Since indentation and silica concentration are not normally distributed, we followed the method of Wilcox [51,52] and applied a robust tests sets on the data. To do a pairwise comparison of the non-ranked but trimmed data (15%) we applied the pairwise comparison test analogous to Dunnett's T3 test [53] in combination with the rank-based Cliff's method [54]. Indentation measurements are made 2–4 times for each phytolith. Each indentation measurement (labeled as indent count, Table 1) is nested in phytolith for statistical analysis.

2.4. Ultrastructure of phytoliths of H. vulgare

The extracted phytoliths of *H. vulgare* [barley] (Fig. 1b) were embedded in epoxy resin as described in [17]. Originally we planed to study ultrastructure of *Temeda triandra* as well; however we failed in embedding the phytoliths. Therefore only barley was used as sampled species. It has larger phytolith and allowed a better handling and measuring the samples. The epoxy-phytolith mixture was filled into a flat silicone rubber. No staining or fixation techniques were used. After hardening, samples were cut with an ultramicrotome (Ultracut E, Reichert-Jung, Leica Microsystems, Wetzlar, Germany) and analysed with a TEM (LEO 906E, LEO, Oberkochen, Germany) at 100 kV. Micrographs were recorded using a computer-linked camera (CCD camera, multi-scan type 794, Gatan, Abingdon, Great Britain) and edited with the software Gatan Microscopy Suite 2.0 (Gatan, Abingdon, UK).

3. Results

3.1. Nano-indentation on phytoliths

The ranges of indentation measurements are shown in Fig. 1e (median, interquartile range (IQR))=1.5*IQR. Mean indentation values of both phytolith populations are very similar (Table 2, $p_{Dunnett}=0.377$, $p_{Cliff}=0.290$). The 10 mg SiO_2/L population of *Themeda triandra* has phytolith indentation values of 2.030 ± 0.882 GPa (mean) being close

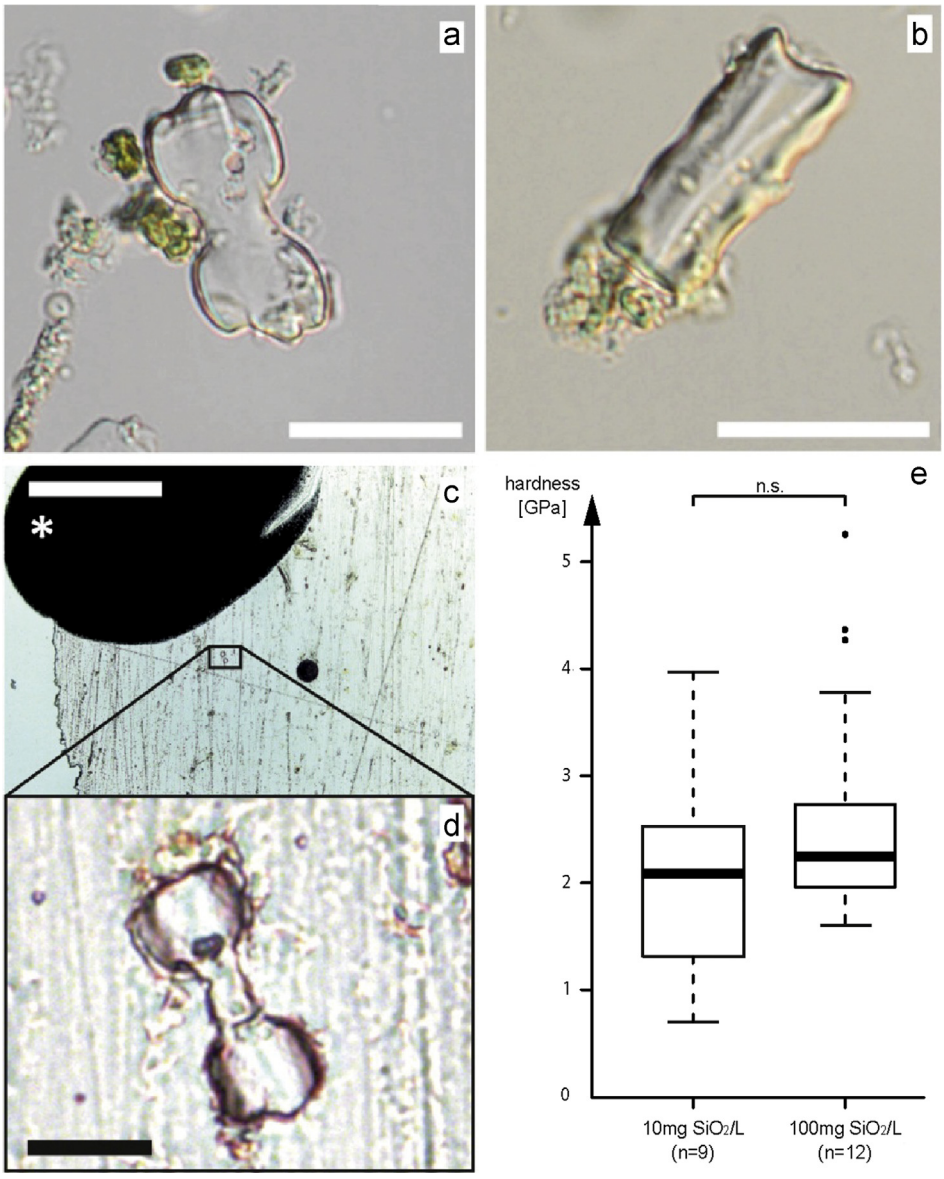

Fig. 1. Nano-indentation measurements of grass phytoliths. Phytoliths of *Themeda triandra* (a) and *Hordeum vulgare* (b) displayed after extraction using the water boiling method (Braune et al. [41]) with some residues of plant tissue. Note the mark of ink (*) used to locate individual phytoliths of *T. triandra* (d). Boxplots (e) showing nano-indentation values based on phytoliths of the silicate controlled populations of *Themeda triandra*. Left: 10 mg (P_10); right: 100 mg (P_100) SiO_2/L. Whiskers include mild outliers (smaller then 4 GPa), extreme outliers (exceeding 4 GPa) identified as individual data points. Note, that differences between 10 mg and 100 mg populations are not significant. Scale: a, b = 25 µm, c = 400 µm, d = 15 µm.

to the 100 mg SiO_2/L population (2.472 ± 0.620 GPa mean). Indentation values (including outliers) range between 0.71 GPa and 3.97 GPa (10 mg SiO_2/L population). In the 100 mg SiO_2/L population the range of the raw values is slightly larger (1.63 GPa to 5.24 GPa) albeit the IQR in the 100 mg SiO_2/L population is smaller (Fig. 1e).

3.2. The Ultrastructure of phytoliths – TEM documentation

The border area of the silica cell which contains the phytolith (Fig. 1a) shows cytoplasma and immediately adjacent to the phytolith (Fig. 2a) a granulated transitional zone [55] (Fig. 17) term this zone as “fibrillary material”. The transitional zone appears to be the growing zone of the phytolith, as silica bodies here are in immediate contact with the transitional zone, where they seem to originate at the outer border of the phytolith. Silica bodies appear amorphous and are partially covered by less electron dense angular bodies, which appear to belong to an inter-body matrix (Fig. 2d). Silica bodies are arranged in densely packed stacks.

These silica bodies are consistently close to 168 nm wide. Individual silica bodies have a variable length that averages 520 nm. We do not observe significantly shorter individual length of silica bodies at the margins of the phytolith, respectively at the proposed zone of formation as reported by Kaufman et al. [55]. In fact we observe that there is large variability in the length, but a high uniformity in width, which equals the thickness of the stacks. Sectioning the

Table 1
List of individual silica phytoliths measured (phytolith ID), silicate available to *Themeda triandra* plants (population), range of indentation depth at individual measurement (indentation depth), number of indentation measurements performed on an individual phytolith specimen (indent count).

phytolith ID	population	indentation depth [nm]	indent count
6A_2	10 mg SiO_2	50–200	3
6A_3	10 mg SiO_2	50–400	4
6A_4	10 mg SiO_2	50–200	4
6A_5_2	10 mg SiO_2	50–150	2
6A_6	10 mg SiO_2	250–500	2
6A_7	10 mg SiO_2	100–300	2
6A_8	10 mg SiO_2	50–150	2
6A_9	10 mg SiO_2	50–200	2
6A_10	10 mg SiO_2	50–200	2
9 total			23
6B_1	100 mg SiO_2	100–250	2
6B_2	100 mg SiO_2	100–300	3
6B_3	100 mg SiO_2	100–200	2
6B_4	100 mg SiO_2	50–150	3
6B_5	100 mg SiO_2	50–150	3
6B_6	100 mg SiO_2	100–200	2
6B_7	100 mg SiO_2	100–250	3
6B_8	100 mg SiO_2	150–300	2
6B_9_1	100 mg SiO_2	50–100	2
6B_9_2	100 mg SiO_2	50–100	3
6B_9_3	100 mg SiO_2	50–100	2
6B_10	100 mg SiO_2	450–600	2
12 total			29

phytolith with a diamond knife for TEM-preparation results in series of artefacts, this shed some light on the ultrastructure. Note the large degree of folding and overlapping resulting from sectioning (Fig. 2b). It should be noted that no fragments of silica bodies are produced when the knife cuts through a phytolith, but instead it shatters the stacks of bodies and causing them to break out of the sectioning plane. In places this results in "empty areas" in the section, which formerly were densely packed with stacks of silica bodies (Fig. 2b). If the course of the sectioning diamond by chance forms a right angle with the stack margins of the silica bodies, as this is the case in the section depicted in Fig. 2b, areas with less artificial displacement are obtained, that allow studying the natural arrangement of silica bodies. This is not the case in the section depicted in Fig. 2a, which shows a more chaotic and diffuse dispersal of silica bodies. This observation indicates that bodies lying in densely packed stacks are only separated along lines of structural weakness that appear to be bound by the inter-body matrix (Fig. 2c-d). The matrix thus appears to be more brittle then the silica body itself and constitutes a mechanical zone of reduced shear force resistance, causing silica bodies to separate when the composit is hit by the knife.

Along the section globular inclusions (Fig. 2b) of 597 nm average size with an electron translucent, non mineralized and unstructured content are distributed within the mass of silica bodies. It should be noted that these inclusions' margins are perfectly smooth and non-angular (Fig. 2c), which indicates, that either silica body stacks developed around these inclusions and individual bodies did not penetrate them, or alternatively, globular inclusions formed after the mass of silica stacks has consolidated. If the latter was true, however, one would expect margins of the globular inclusions to not precisely cut silica bodies (as observed) but display a fuzzier marginal zone as a result of presumably corrosive action. There is a thin layer of light, crystal like "inter-body matrix", which lines the gaps between the silica bodies (Fig. 2d). This matrix appears to be crystalline, because of the angularity of fragments produced when hitting it with the knife (Fig. 2e). The matrix is a bonding layer jacketing every single silica body and bonding it to its neighbour. If this matrix is indeed crystalline, as it appears, this would explain its comparatively brittle behaviour if loaded by the diamond knife and explain the disintegration of the phytolith as described above. A phytolith would then appear as a highly organized and highly oriented composit of at least 3 different components, amorphous silica bodies and non-mineralized globular inclusions bound together by a crystalline matrix.

4. Discussion

4.1. Phytolith ultrastructure

TEM analysis shows that phytoliths are highly anisotropic composites consisting of oriented silica bodies. The formation of a phytolith according to Kaufman, et al. [32] begins in the intercalary meristem, where after cell division the primary cell wall is newly formed from the middle lamella [56] and the initial storage of silicates would be conceivable in this step. The morphology and layout of the silica bodies as seen in the TEM micrographs are consistent with descriptions by Sangster and Parry [56] and Kaufman, et al. [32] The observed heterogeneity in the examined phytoliths is attributed to a gradual, centripetal growth along undifferentiated fibrillar elements.

Table 2
Mean nano-indentation values (H) and statistics of the two silicate (SiO_2) controlled populations (dataset) of *Themeda triandra*. Abbreviations: SD = standard deviation, Dunnett = pair-wise comparison test analogous to Dunnett's T3 test (t = test value, df = degree of freedom, p = signinicance level), Cliff = Cliff's method (ph = test value, pl = lower 95% confidence intervall, pu = upper 95% confidence intervall, p = signinicance level, pc = critical significance level).

Dataset		Descriptive statistics				Dunnett			Cliff			
	SiO_2 [mg]	n	H [GPa]	SD	t	df	p	ph	pl	pu	p	pc
1	10	23	2.030	0.882	0.935	8.144	0.377	0.657	0.377	0.859	0.290	0.050
2	100	29	2.472	0.620								

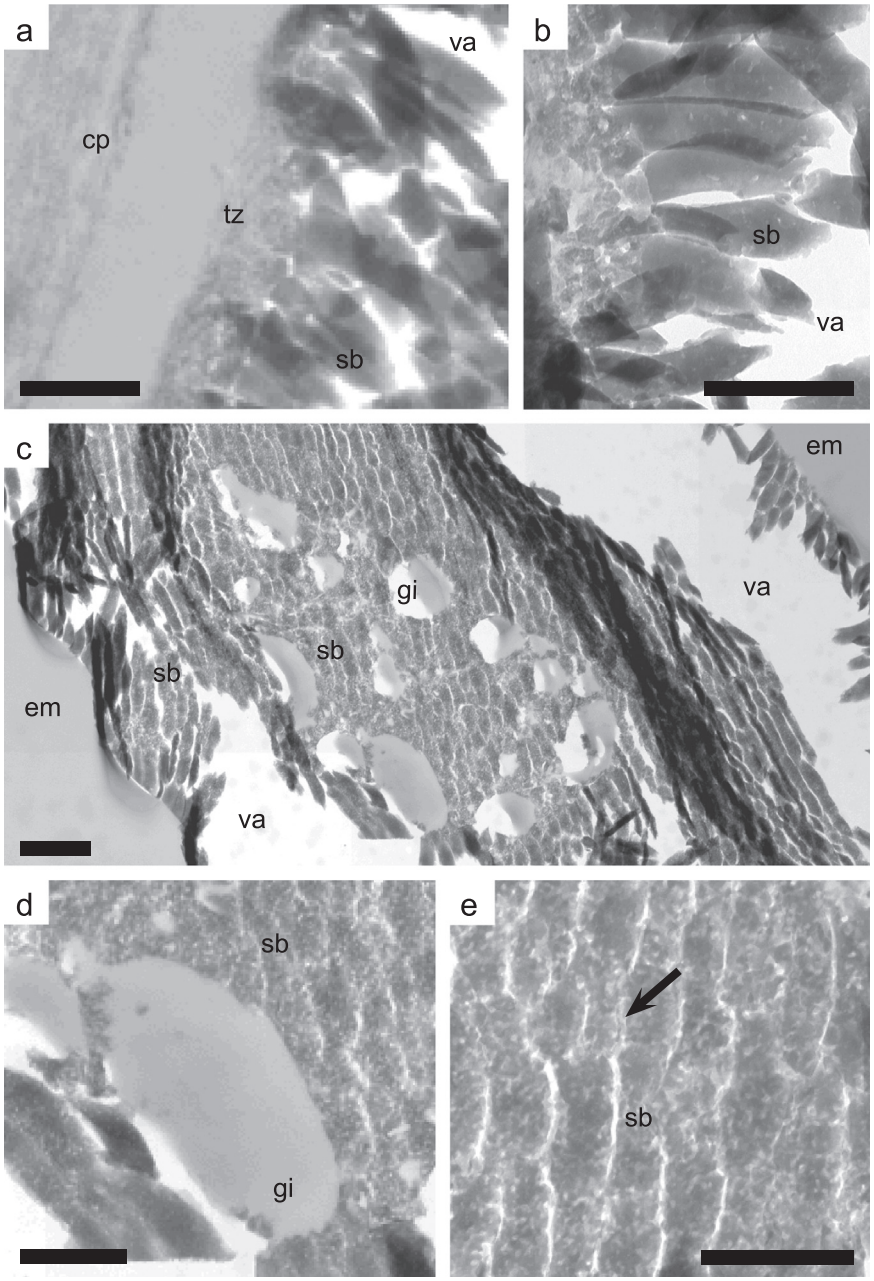

Fig. 2. TEM micrographs indicating phytolith ultrastructure. No staining and no fixation used for TEM micrographs of a phytolith of *Hordeum vulgare* (a) Border area of a phytolith; left section: cytoplasma (cp) of the silica cell with a granulated transitional zone (tz); Right section: silica bodies (sb), partially still in contact with the transitional zone. (b) The translucent areas (va = void artefact) in the micrograph are sectioning artefacts. (c) Overview of a portion of the phytolith bordered by embedding epoxy matrix (em). Note, that there is no surrounding cytoplasma preserved, due to previous preparation. In the center of the micrograph, sectioning artefacts are minor and the undisturbed ultrastructure can be seen. Globular inclusion (gi) with non mineralized homogenous content (light grey; pushed to the right as a sectioning artefact). (d) Note that the margin of the globular inclusion is perfectly smooth, non-angular and that its course appears to not relate to the outlines of the silicate bodies. (e) Thin layer of light, crystal like "inter-body matrix" (arrow) lines the gaps between the silicate bodies, and it appears as if this matrix was a crystalline bonding layer jacketing every single silicate body and bonding it to its neighbour. Scale: a, c, d: 500 nm, b: 1000 nm.

The gaps between the densely packed stacks of silica bodies seen on TEM micrographs are interpreted to be artifacts from the sectioning process. They do, however, highlight lines of structural weakness that obviously are prone to mechanical stress. This supports the notion that stack margins are in fact structural properties independent of the sectioning procedure. Therefore we would expect a phytolith to behave similarly when loaded as dietary components in the occlusal gap of an herbivorous mammal. It would either be disintegrated into isolated silica bodies of the above mentioned dimensions or, alternatively, when load is more perpendicular with lines of stack margins, into larger fragments.

Jones and Milne [43] as well as Lanning, et al. [57] determine the silicate deposits in plants by means of X-ray diffraction as amorphous opal and α-quartz bodies (polymorphs), but unlikely as silicate gel as hypothesized by

Kaufman et al. [32]. Our results partly support the first two studies [43,57], as the phytoliths we measured display a composit of highly organised crystal-like silicate bodies. The inter-body matrix is interpreted as an even more crystalline structure, but might also be a transitional stage between silica gel and fully crystallized bodies.

4.2. Nano-indentation on phytoliths

Indentation values of phytoliths are slightly higher and more variable in the 10 mg SiO_2/L population of *Themeda triandra* than in the on 100 mg SiO_2/L population, although these differences are not significant. Regarding indentation hardness measurements and its technical limitations, it can be critically argued, that because of the needle like shape indentor tip the indenter would hit a phytolith like a needle would penetrate between the bristles of a brush and it would possibly rather test for cohesion of the silica bodies (via the inter-body matrix), not indicating the hardness of the bodies themselves. However we do not have an alternative test at hand and would therefore not speculate further. For further studies we would recommend a nano-indentaion test procedure that affects silica body geometry in a minor way. Another limitation that has to be taken into account might be the globular inclusions (Fig. 2b, c) we found, which are possible remains of lipid droplets [32] might influence indentation-depth measurements if directly penetrated by the nano-indenter and lead to fluctuations in stiffness during CSM hardness measurement.

In comparision to a former study by Lucas et al. [16], who also performed nano-indentation on phytoliths, results for hardness values in the present study fall into the same range (2.56 ± 0.81 GPa). Lucas et al. [16] investigated grass phytoliths of *Ampelodesmos mauritanicum* (Poir.) T. Durand & Schinz extracted by wet oxidation, but gave no information on the indentation depths that were used for averaging. Due to this inconsistency in data structure, the comparison with their results is difficult.

Besides of performing phytolith hardness determinations using other methods of hardness testing, Lucas et al. [16], Sanson et al. [18], Baker et al. [5] Erickson [19] do not mention the origin of plant material in their studies. The present work thus is the first to provide information on growth conditions of the test species (10 and 100 mg SiO_2/L mg), number of phytoliths, indents obtained and precise descriptions of the procedure. This should help scholars to reproduce and complement data critical to our understanding of phytolith hardness and its bearing on habitat conditions and plant animal interaction. Beside the above mentioned technical limitations our results confirm that the silicate concentration in the substrate does not affect the hardness of the phytoliths and thus suggests that (at least for the tested species and silica concentrations used) phytolith nano-indentation hardness is independent of silica availability in the substrate. This may not immediately be translated into complete independence of phytolith hardness and other habitat properties. However, the variability in hardness may be responsible for at least some influence of the substrate. Hence, if any substrate parameter should influence phytolith hardness, silica availability should certainly play a role.

4.3. Phytolith production in plant tissues

The phytolith-formation cannot be free of environmental influences. With increased water-availability, silicification occurs not only in epidermal short cells but also in epidermal long cells [58]. Schaller, et al. [59] found that phytolith quantity in the leaf tissue can be increased by supplementary silicate provisioning [59]. The abrasiveness of the leaves is also found to be increased [6]. Our results point to a similar direction like Schaller, et al. [59]. It clearly indicates that a higher silicate concentration in the substrate does not lead to harder phytoliths but rather to a larger quantity of phytoliths. Hence, the results of our study confirm the findings of [59] and explain the increased abrasiveness as indicated by [6]. Assuming phytoliths are constituted by amorphous opal (SiO_2*nH_2O) with an undetermined water content, there would be enough water available to prevent full crystallisation to harder α-quartz phytoliths in living cells, even during water stress. Water stress should thus not necessarily increase the hardness of phytoliths in plant tissue even if the designated silica cells provide limited space for silification [32,55].

4.4. Abrasiveness of plant tissues and its bearing on animal-plant interaction

The cause of tooth wear has long been attributed to phytoliths. This is mainly because Baker et al. [5] found silicate phytolith to be harder then sheep tooth enamel. The study has thus for a long time dominated the discussion on dental feeding traits in mammals, that were widely considered the result of plant-animal co-evolution [1,3,35,60–63]. However our knowledge about how the variety of mineralized internal plant abrasives (e.g. beside diverse silica phytolith oxalates are of importance too [64,65]) is still limited and need to be studied in more detail. Further one could argue that an increased silica concentration in the substrate leads to larger phytolith quantities and increasing damage risks in the protein bonds between the hydroxyapatite crystals of the enamel as suggested by Xia, et al. [66,67]. Sanson et al. [18], Lucas et al. [16] and Erickson [19] provided softer phytolith hardness data and thus changed this notion. Extrinsic dust and soil particles are considered to play a more important role in explaining tooth wear [68]. In recent years increasing abrasiveness by dust loads in dry habitats is confirmed by evidence from field studies in free-ranging Arabian gazelles [69,70] based on feeding and tooth wear observations.

In feeding experiments with rabbits and guinea pigs, Müller et al. [71,72] found that both, mineral soil particles and plant ingredients with internal phytoliths can abrade teeth of herbivorous mammals, but mineral soil particles have a greater effect on the tooth-wear. For sheep, Merceron et al. [73] found contradicting results and conclude that experimentally added external abrasives (less than 1% dry matter intake) do not

influence tooth wear significantly, while inherent material properties of the forage are reflected in tooth wear.

5. Conclusions

The nano-indentation measurements of *Themeda triandra* phytoliths in this study support former finding that phytoliths are softer then tooth enamel, but still remain a source of abrasiveness in herbivorous diets. It was found, that phytoliths of *Hordeum vulgare* measured display a composit of highly organised crystal-like silicate bodies. The inter-body matrix is interpreted as an even more crystalline structure, but might also be a transitional stage between silica gel and fully crystallized bodies. For future studies we highly recommend further developments of a nano-indentaion test procedure that affects silica body geometry in a minor way and takes into account that penetrating the phytolith by the nano-indenter might lead to fluctuations in stiffness during CSM hardness measurement. We found that silicate concentration in the substrate does not affect the hardness of the phytoliths and thus suggests that (at least for the tested species and silica concentrations used) phytolith nano-indentation hardness is independent of silica availability in the substrate.

Acknowledgements

This research was supported by the “Deutsche Forschungsgemeinschaft” (DFG, German Research Foundation, (KA 1525/8-1, KA 1525/8-2) and is publication no. 82 of the DFG Research unit 771. We thank Gerhard Kalinka and Michael Griepentrog, (both Federal Institute for Materials Research and Testing, Berlin, Germany) for their support in acquiring nano-indentation measurements. Martina Bistritz and Rüdiger Sernow (both Federal Institute for Materials Research and Testing, Berlin, Germany) are acknowledged for their assistance with preparation and handling samples.

References

[1] T.M. Kaiser, D.W.H. Müller, M. Fortelius, E. Schulz, D. Codron, M. Clauss, Hypsodonty and tooth facet development in relation to diet and habitat in herbivorous ungulates: implications for understanding tooth wear, Mammal. Rev. 43 (2013) 34–46.

[2] M.C. Mihlbachler, F. Rivals, N. Solounias, G.M. Semprebon, Dietary change and evolution of horses in North America, Science 331 (2011) 1178–1181.

[3] N. Solounias, G. Semprebon, Advances in the reconstruction of ungulate ecomorphology and application to early fossil equids, Am. Mus. Novit. 3366 (2002) 1–49.

[4] P. Ungar, G. Merceron, R. Scott, Dental microwear texture analysis of Varswater bovids and early Pliocene paleoenvironments of Langebaanweg, Western Cape Province, South Africa, J. Mamm. Evol. 14 (2007) 163–181.

[5] G. Baker, L.H.P. Jones, I.D. Wardrop, Cause of wear in sheep's teeth, Nature 184 (1959) 1583–1584.

[6] F.P. Massey, A.R. Ennos, S.E. Hartley, Silica in grasses as a defence against insect herbivores: contrasting effects on folivores and a phloem feeder, J. Anim. Ecol. 75 (2006) 595–603.

[7] F.P. Massey, K. Massey, R.A. Ennos, H.S. E, Impacts of silica-based defences in grasses on the feeding preferences of sheep, Basic Appl. Ecol. 10 (2009) 622–630.

[8] S.J. McNaughton, J.L. Tarrants, Grass leaf silicification: natural selection for an inducible defense against herbivores, Proc. Natl. Acad. Sci. 80 (1983) 790–791.

[9] S.J. McNaughton, J.L. Tarrants, M.M. McNaughton, R.H. Davis, Silica as a defence against herbivory and a growth promotor in African grasses, Ecology 66 (1985) 528–535.

[10] M. Vicari, D.R. Bazely, Do grasses fight back? The case for antiherbivore defense, Tr. Ecol. Evol. 8 (1993) 137–141.

[11] J. Xia, J. Zheng, D. Huang, Z.R. Tian, L. Chen, Z. Zhou, P.S. Ungar, L. Qian, New model to explain tooth wear with implications for microwear formation and diet reconstruction, Proc. Natl. Acad. Sci. USA 112 (2015) 10669–10672.

[12] D. Rabenold, O.M. Pearson, Abrasive, silica phytoliths and the evolution of thick molar enamel in primates, with implications for the diet of *Paranthropus boisei*, PloS ONE 6 (2011) e28379.

[13] D. Rabenold, O.M. Pearson, Scratching the surface: a critique of Lucas et al. (2013)'s conclusion that phytoliths do not abrade enamel, J. Hum. Evol. 74 (2014) 130–133.

[14] P.W. Lucas, R. Omar, K. Al-Fadhalah, A.S. Almusallam, A.G. Henry, S. Michael, L.A. Thai, J. Watzke, D.S. Strait, A. van Casteren, A. G. Atkins, Tooth wear: a response to “Scratching the surface: a critique of Lucas et al. (2013)'s conclusion that phytoliths do not abrade enamel” [J. Hum. Evol. 74 (2014) 130–133], J. Hum. Evol. 102 (2017) 75–77.

[15] D. Rabenold, A scratch by any other name: a comment on Lucas et al.'s reply to “Scratching the surface: a critique of Lucas et al. (2013)'s conclusion that phytoliths do not abrade enamel” [J. Hum. Evol. 74 (2016) 130–133], J. Hum. Evol. 102 (2017) 78–80.

[16] P.W. Lucas, R. Omar, K. Al-Fadhalah, A.S. Almusallam, A.G. Henry, S. Michael, L.A. Thai, J. Watzke, D.S. Strait, A.G. Atkins, Mechanisms and causes of wear in tooth enamel: implications for hominin diets, J. R. Soc. Int. 10 (2013).

[17] T.M. Kaiser, C. Braune, G. Kalinka, E. Schulz-Kornas, Nano-indentation of native phytoliths and dental tissues: implications for herbivore-plant combat and dental wear proxies, Evolutionary Systematics (submitted).

[18] G.D. Sanson, S.A. Kerr, K.A. Gross, Do silica phytoliths really wear mammalian teeth?, J. Arch. Sci. 34 (2007) 526–531.

[19] K.L. Erickson, Prairie grass phytolith hardness and the evolution of ungulate hypsodonty, Hist. Biol. 26 (2013) 737–744.

[20] P.W. Lucas, Av Casteren, K. Al-Fadhalah, A.S. Almusallam, A. G. Henry, S. Michael, J. Watzke, D.A. Reed, T.G.H. Diekwisch, D. S. Strait, A.G. Atkins, The role of dust, grit and phytoliths in tooth wear, Ann. Zool. Fenn. 51 (2014) 143–152.

[21] P.W. Lucas, R. Omar, K. Al-Fadhalah, A.S. Almusallam, A.G. Henry, S. Michael, L.A. Thai, J. Watzke, D.S. Strait, A.G. Atkins, Mechanisms and causes of wear in tooth enamel: implications for hominin diets, J. R. Soc. Interface 10 (2013).

[22] P.W. Abrahams, S. J, Soil ingestion by sheep grazing the metal enriched floodplain soils of mid-Wales, Environ. Geochem. Health 25 (2003) 17–24.

[23] T.W. Cutress, W.B. Healy, Wear of sheep's teeth II. Effects of pasture juices on dentine, N. Z. J. Agric. Res. 8 (1965) 753–762.

[24] W.B. Healy, T.G. Ludwig, Wear of sheep's teeth: i The role of ingested soil, N. Z. J. Agric. Res. 8 (1965) 737–752.

[25] T.G. Ludwig, W.B. Healy, C.T. W, Wear of sheep's teeth III. Seasonal variation in wear and ingested soil, N. Z. J. Agric. Res 9 (1966) 157–164.

[26] N.D. Grace, L. P, M.J. Hedley, The effect of a temporal change in ingestion rates of fluorine (F) in soil on the concentration of F in serum and bone of young sheep, N. Z. Veter-. J. 55 (2007) 279–286.

[27] W.N. Beyer, E.E. Connor, S. Gerould, Estimates of soil ingestion by wildlife, J. Wildl. Manag. 58 (1994) 375–382.

[28] F.A. Sneva, H.F. Mayland, M. Vavra, Soil ingestion by ungulates grazing a sagebrush-bunchgrass range in eastern Oregon 1983 Progress Report - Research in Rangeland Management, Agricultural Experiment Station,

Oregon State University, Corvallis in cooperation with Agricultural Research Service, U.S. Department of Agriculture, Corvallis, 1983.
[29] J. Hummel, E. Findeisen, K.H. Südekum, I. Ruf, T.M. Kaiser, M. Bucher, M. Clauss, D. Codron, Another one bites the dust: faecal silica levels in large herbivores correlate with high-crowned teeth, Proc. R. Soc. B: Biol. Sci. 278 (2010) 1742–1747.
[30] M.J. Hodson, P.J. White, A. Mead, M.R. Broadley, Phylogenetic variation in the silicon composition of plants, Ann. Bot. 96 (2005) 1027–1046.
[31] T.L. Simpson, B.E. Volcani, Silicon and Siliceous Structures in Biological Systems, Springer Verlag, Berlin, 1981.
[32] P.B. Kaufman, P. Dayanandan, Y. Takeoka, J.D. Bigelow, J.D. Jones, R. Iler, Silica in shoots of higher plants, in: T.L. Impson, B.E. Volcani (Eds.), Silicon and Siliceous Structures in Biological Systems, Springer-Verlag, New York, 1981, pp. 409–449.
[33] P.B. Kaufman, L.B. Petering, J.G. Smith, Ultrastructural development of cork-silica cell pairs in Avena internodal epidermis, Bot. Gaz. 1 (1970) 173–185.
[34] E.E. Farmer, Leaf Defense, Oxford University Press, Oxford, 2014.
[35] S.J. McNaughton, J.L. Tarrants, Grass leaf silicification: natural selection for an inducible defense against herbivores, Proc. Natl. Acad. Sci. 80 (1983) 790–791.
[36] S.E. Hartley, R.N. Fitt, E.L. McLarnon, R.N. Wade, Defending the leaf surface: intra- and inter-specific differences in silicon deposition in grasses in response to damage and silicon supply, Front. Plant Sci. 6 (2015).
[37] F.P. Massey, A. Roland Ennos, S.E. Hartley, Herbivore specific induction of silica-based plant defences, Oecologia 152 (2007) 677–683.
[38] R.L. Casebeer, G.G. Koss, Food habits of wildebeest, zebra, hartebeest and cattle in Kenya Masailand, East Afr. J. 8 (1970) 25–36.
[39] M.L. Owaga, The feeding ecology of wildebeest and zebra in Athi-Kaputei plains, East Afr. Wildl. J. 13 (1975) 375–383.
[40] D.R.M. Stewart, J. Stewart, Food preference data by faecal analysis for African plains ungulates, Zool. Afr. 15 (1970) 115–129.
[41] C. Braune, R. Lieberei, D. Steinmacher, T.M. Kaiser, A simple microwave extraction method for the isolation and identification of plant opal phytoliths, Biologia 67 (2012) 927–930.
[42] L.H.P. Jones, K.A. Handreck, Studies of silica in the oat plant, Plant Soil 23 (1965) 79–96.
[43] L.H.P. Jones, A.A. Milne, Studies of silica in the oat plant: I. Chemical and physical properties of the silica, Plant Soil 18 (1963) 207–220.
[44] J. Pironon, J.D. Meunier, A. Alexandre, R. Mathieu, L. Mansuy, A. Grosjean, E. Jarde, Individual characterization of phytoliths: experimental approach and consequences on paleoenvironment understanding, in: J.D. Meunier, F. Colin (Eds.), Phytoliths: Applications in Earth Sciences and Human History, Balkema Publishers, Lisse, 2001, pp. 329–341.
[45] R.D.C. Team, R: A Language and Environment for Statistical Computing, R Foundation for Statistical Computing, Vienna, Austria, 2011.
[46] S. Højsgaard, K. Wright, A.A. Leidi, doBy: Groupwise computations of summary statistics, general linear contrasts and other utilities, R package version 4.0.6, 2010.
[47] H. Bengtsson, R.utils: Various programming utilities, R package version 1.4.0, 2010.
[48] T.J. Luciani, RSvgDevice, A. SVG, graphics device, R package version 0.6.4.1, 2009.
[49] H.-P. Suter, xlsReadWrite: Natively read and write Excel files, R package version 1.5.1, 2010.
[50] R.R. Wilcox, F.D. Schönbrodt, The WRS package for robust statistics in R, R package version 0.12.1, 2010.
[51] R.R. Wilcox, Introduction to Robust Estimation and Hypothesis Testing, (2005) 1-588.
[52] R.R. Wilcox, Applying Contemporary Statistical Techniques, (2003) 1-608.
[53] C.W. Dunnett, Pairwise multiple comparisons in the unequal variance case, J. Am. Stat. Assoc. 75 (1980) 796–800.
[54] N. Cliff, Ordinal Methods for Behavioral Data Analysis, Lawrence Erlbaum, Mahwah, New Jersey, 1996.
[55] P.B. Kaufman, L.B. Petering, J.G. Smith, Ultrastructural development of silica-cork cell pairs in Avena internodal epidermis, Bot. Gaz. 173 (1970) 173–185.
[56] A.G. Sangster, D.W. Parry, Ultrastructure of silica deposits in higher plants, in: T.L. Simpson, B.E. Volcani (Eds.), Silicon and Siliceous Structures in Biological Systems, Springer-Verlag, New York, 1981, pp. 383–407.
[57] F.C. Lanning, B.W.X. Ponnaiya, C.F. Crumpton, The chemical nature of silica in plants, Plant Physiol. 33 (1958) 339–343.
[58] M. Madella, M.K. Jones, P. Echlin, A. Powers-Jones, M. Moore, No title, Quat. Int. 193 (2009) 32–40.
[59] J. Schaller, C. Brackhage, M.O. Gessner, E. Bäuker, E.G. Dudel, Silicon supply modifies C:n:p stoichiometry and growth of *Phragmites australis*, Plant Biol. 14 (2012) 392–396.
[60] M. Fortelius, N. Solounias, Functional characterization of Ungulate molars using the abrasion-attrition wear gradient: a new method for reconstructing palaeodiets, Am. Mus. Novit. 3301 (2000) 1–36.
[61] G. Merceron, E. Schulz, L. Kordos, T.M. Kaiser, Paleoenvironment of *Dryopithecus brancoi*at Rudabánya, Hungary:evidence from dental meso- and micro-wear analyses of large vegetarian mammals, J. Hum. Evol. 53 (2007) 331–349.
[62] C.A.E. Strömberg, Evolution of hypsodonty in equids: testing a hypothesis of adaptation, Palaeobiology 32 (2006) 236–258.
[63] P.S. Ungar, Mammal Teeth – Origin, Evolution and Diversity, The John Hopkins University Press, Baltimore, 2010.
[64] D.R. Danielson, K.J. Reinhard, Human dental microwear caused by calcium oxalate phytoliths in prehistoric diet of the Lower Pecos Region, Texas, Am. J. Phys. Anthropol. 107 (1998) 297–304.
[65] B. Libert, V.R. Franceschi, Oxalate in crop plants, J. Agric. Food Chem. 35 (1987) 926–938.
[66] J. Xia, Z.R. Tian, L. Hua, L. Chen, Z. Zhou, Q. L, P.S. Ungar, Enamel crystallite strength and wear: multiscale nanobonding responses to chewing loads, J. R. Soc. Int. 14 (2017) 20170456.
[67] J. Xia, J. Zheng, D. Huang, Z.R. Tian, L. Chen, Z. Zhou, P.S. Ungar, L. Qian, New model to explain tooth wear with implications for microwear formation and diet reconstruction, Proc. Natl. Acad. Sci. USA 112 (2015) 10669–10672.
[68] J. Damuth, C.M. Janis, On the relationship between hypsodonty and feeding ecology in ungulate mammals, and its utility in palaeoecology, Biol. Rev. Camb. Philos. Soc. 86 (2011) 733–758.
[69] E. Schulz, S. Fraas, T.M. Kaiser, P. Cunningham, K. Ismail, T. Wronski, Food preferences and tooth wear in sand gazelle (*Gazella marica*), Mamm. Biol. 78 (2013) 55–62.
[70] T. Wronski, E. Schulz-Kornas, The Farasan Gazelle – a frugivorous browser in an arid environment?, Mamm. Biol. 80 (2015) 87–95.
[71] J. Müller, M. Clauss, D. Codron, E. Schulz, J. Hummel, M. Fortelius, P. Kircher, J.-M. Hatt, Tooth length and incisal growth and wear in guinea pigs (*Cavia porcellus*) fed diets of different abrasiveness, Anim. Physiol. Anim. Nutr. (2014).
[72] J. Müller, M. Clauss, D. Codron, E. Schulz, J. Hummel, M. Fortelius, P. Kircher, J.-M. Hatt, Growth and wear of incisor and cheek teeth in domestic rabbits (*Oryctolagus cuniculus*) fed diets of different abrasiveness, J. Exp. Zool. A 321 (2014) 283–298.
[73] G. Merceron, A. Ramdarshan, C. Blondel, J.R. Boisserie, N. Brunetiere, A. Francisco, D. Gautier, X. Milhet, A. Novello, D. Pret, Untangling the environmental from the dietary: dust does not matter, Proc. R. Soc. B 283 (2016) 20161032.